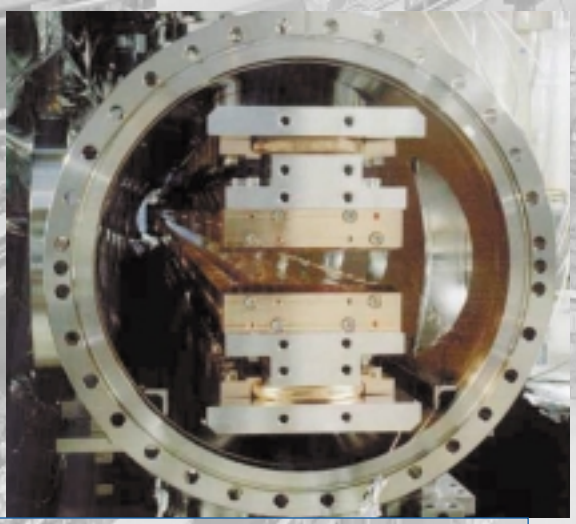

Accelerator Operation and Development

Accelerator Operation & Development

Light Source Division

Introduction

Accelerator-related activities at SRRC have focussed on improving reliability, increasing beam stability, and improving machine performance. In order to meet these goals, light source operations and machine maintenance are constantly being improved, and a number of machine upgrades are under way.

Accelerator Operation

The light source was scheduled to operate continuously throughout year 2000 except for one three-day maintenance shutdown every month, plus occasional long shutdowns for equipment installation as needed. The light source up time for users was about 96%, as shown in *Figure 1*. In order to minimize the disturbance to user operations, the maintenance schedule will be changed into a one-week shutdown every two months starting in 2001.

During year 2000, the operation of the storage ring was interrupted by unknown beam trips about once a day. After improving the power line grounding system, redistributing the power loads of the accelerator subsystems, and improving the stability of the electrical power supplied to the 500 MHz signal generator, the average number of beam trips was greatly reduced to only once a month.

Beam Dynamics

Changing the Insertion-device Gaps during User Operation

The dynamic orbit corrections using follow-gap end

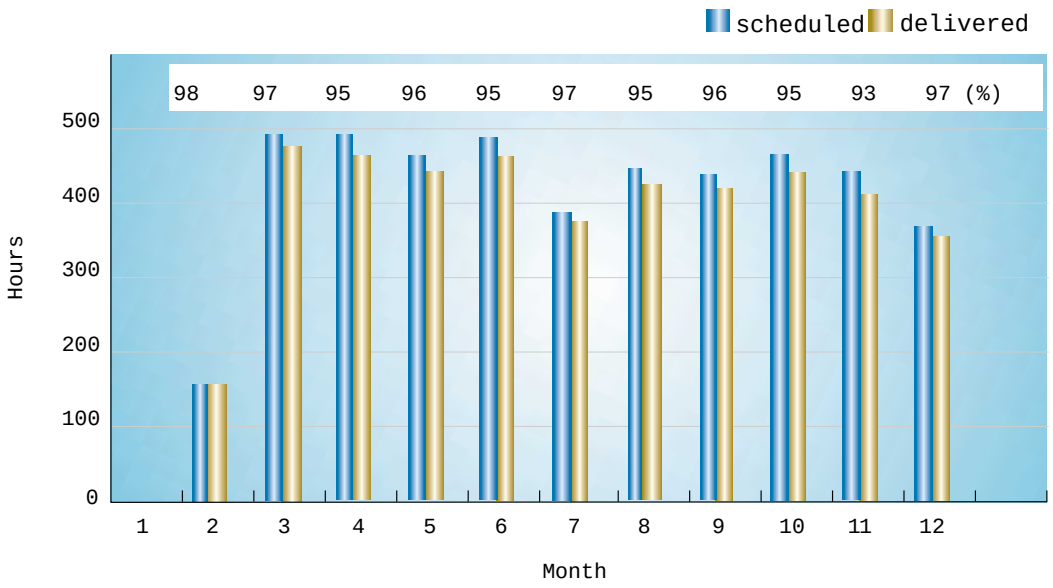

Figure 1 The machine statistics of user shifts in year 2000.

correctors and digital global orbit feedback (during gap changes of U5, EPU, and U9) demonstrate reasonably good performance during routine operation. The orbit excursions during gap changes are kept within 5 μm over the entire tuning range, as shown in *Figure 2 ~ Figure 5*. Presently, the gaps of these insertion devices are changed during one-third of the user shifts.

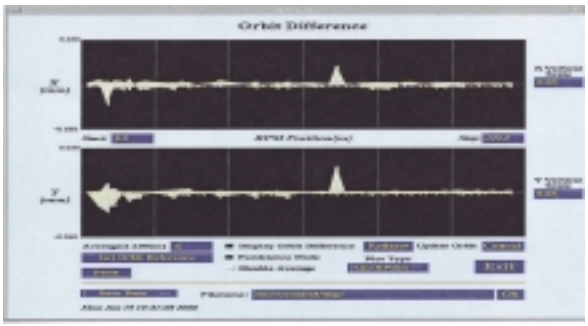

Figure 2 No ID gap change, Orbit feedback ON.

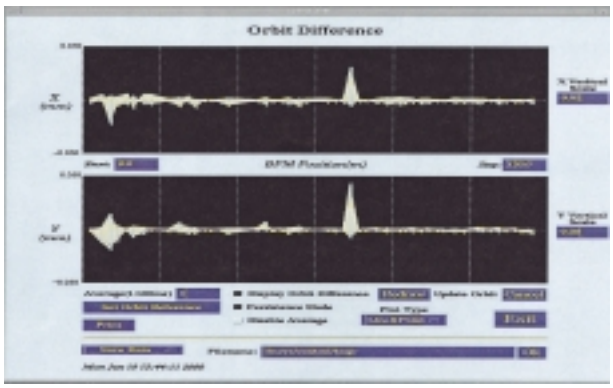

Figure 3 U5 gap change: 55 mm --> 18.5 mm --> 55 mm.

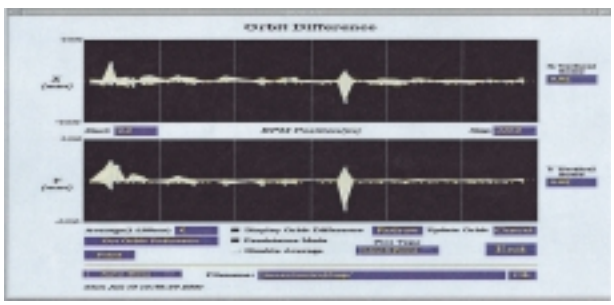

Figure 4 EPU gap change: 20 mm --> 60 mm --> 20 mm.

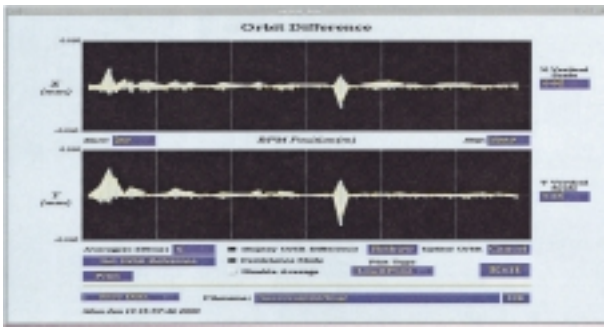

Figure 5 EPU phase change (one cycle).

Beam Manipulation with Parametric Resonance

During routine operations, suppression of longitudinal coupled-bunch instabilities is achieved by employing rf-gap-voltage modulation at about double the synchrotron frequency, as shown in *Figure 6 and Figure 7*. In order to understand the detailed mechanism, analytical calculations and numerical tracking simulations are being carried out. The calculations are consistent with the experimental results.

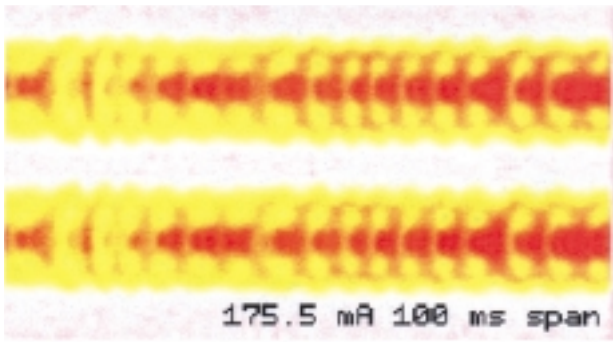

Figure 6 Beam spectrum without rf gap voltage modulation.

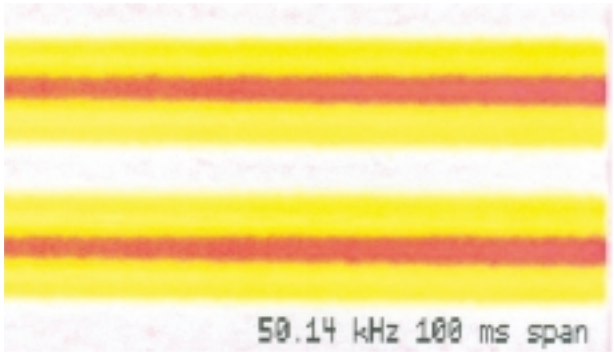

Figure 7 Beam spectrum with rf gap voltage modulation.

Superconducting Wiggler Effects

Single-particle tracking calculations which taking into account the high magnetic fields of a superconducting wavelength shifter (SCWLS) and a superconducting multipole wiggler (SCMW) are being carried out. Calculations show that the dynamic aperture is acceptable with the SCWLS alone, as shown in *Figure 8 and Figure 9*. A detailed study to optimize the operational lattice is under way.

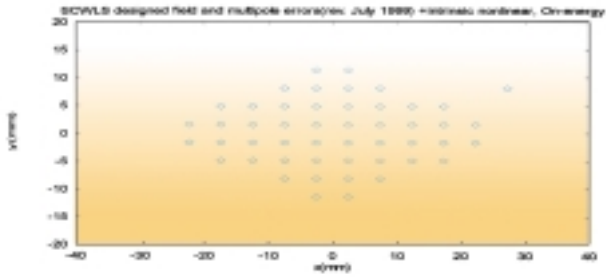

Figure 8 Dynamic aperture (1000 turn tracking) with a 6-T superconducting wavelength shifter.

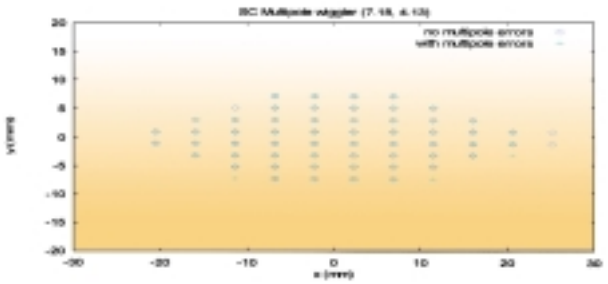

Figure 9 Dynamic aperture (1000 turn tracking) with a 5-T, 19-pole superconduting multipole wiggler.

Instrumentation and Control

Control System

A new control system server computer was installed in May. It runs in parallel with the existing control server, and it has enhanced the fault tolerance of the control system.

The commercially available software "Matlab" is being used to develop control toolboxes for accessing database information and for measuring beam parameters. These include machine lattice measurement, orbit feedback, beam size and lifetime estimation, beam-based alignment, and tune measurement. These toolboxes are under development and will provide an efficient environment for accelerator diagnostics.

Integrating the control system of the superconducting wavelength shifter with that of the superconducting rf cavity will be important to future operations. Various hardware and software tests have been carried out in the past year, in order to meet the installation schedules of the two projects - 2001 and 2002, respectively.

BPM and Orbit Feedback Improvement

A systematic investigation of possible factors affecting BPM performance has been carried out. The measurement resolution for all BPMs will be improved to 1μm this year.

The global orbit feedback system is in routine operation. It has the capability to compensate for orbit perturbations caused by gap and phase changes of insertion devices during user shifts. The closed-loop bandwidth is about 10 Hz, and the system is adequate for handling changes of insertion device gap and phase, at speeds up to 1 mm/sec. New generation DSP boards are being evaluated, because it would be desirable to replace the existing DSP boards, in order to provide greater flexibility of the orbit feedback system.

Electron Beam Instrumentation

Recently, a pseudo-turn-by-turn BPM (PTTBPM) system, equipping all BPMs with turn-by-turn capability, has passed its preliminary tests at the SRRC storage ring. This system is based on ESRF's 'Le Mulle-Tour' BPM (with some modification) and on a similar system at CESR. An upgraded BPM system will permit the efficient retrieval of diagnostic information and storage ring lattice parameters. If budgets permit, all BPMs will be upgraded during the coming year.

Power Supply

The key subcomponent of the booster's pulsed power supply is a thyratron tube and its trigger-pulse generator. The existing pulse driver used for the booster extraction kicker is a general-purpose commercial pulse driver, and pulse reflection and ringing have often caused damage to the power MOS in the driver circuitry. An in-house-designed pulse driver configuration was proposed for solving this problem. The test results were encouraging. They show that the new driver achieves less than 0.5 ns jitter throughout a test period of 4 hours. This unit (SRRC-1000) is now operating in booster ring to drive the extraction kicker. The circuit configuration of the SRRC-1000 thyratron driver is shown in *Figure 10*. Performance comparison between the commercial DEI-1000 pulser driver and the SRRC-1000 pulser is shown in *Figure 11*.

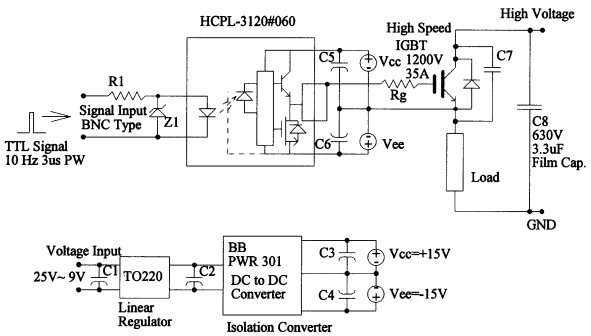

Figure 10 Configuration of new thyratron pulse driver.

Radiofrequency (RF) System

In order to maintain high reliability of the rf system, a thorough checkout of rf components during regular maintenance were carried out. The degraded components were replaced immediately whenever there was a sign of possible threat to routine operation. Most of the replaced components were high power related, such as transformer, saturable reactor, klystron heater power supply, and rf ceramic window.

(a)

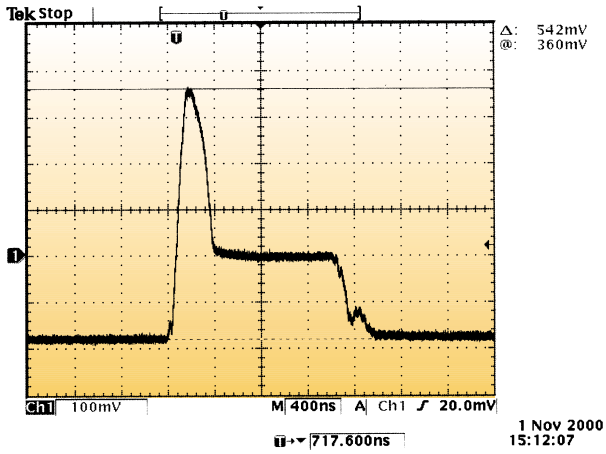

(b)

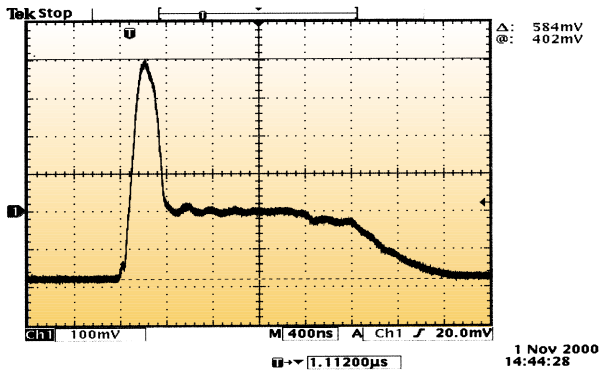

Figure 11 (a) High voltage pulse signal measured at grid 2 of CX1159 with DEI-100 pulser.
(b) High voltage pulse signal measured at grid 2 of CX1159 with SRRC-1000. (Scale :1V=1000V).

Preparation for the Commissioning of the Superconducting Cavity

Fabrication of the niobium cavity is under way. After the construction of this unit, it will be high power tested at Cornell University and then delivered to SRRC in September 2002. The first engineering review meeting was held in November 2000, and the second meeting will be held in winter of 2001.

In order not to interrupt storage-ring operations during the commissioning of the superconducting cavity in 2002, an extra transmitter will be needed to provide the required rf power. Due to budgetary limitations, a spare transmitter was built in house by reproducing the existing units using spare parts. This work was

completed in August, and the new unit has been tested at its full power of 60 kW with a dummy load.

Beam test of the direct feedback loop for SRF low-level electronics has been carried out with stored beam current up to 200 mA. Significant reduction of heavy beam loading effects has been observed by decreasing the cavity gap voltage. The cross talk between amplitude and phase loops of the low level rf system was observed for beam current above 130 mA. Replacing the amplitude and phase loops by an I/Q modulator will be tested in 2001.

Quench detecting circuit for the cryogenic electronics has been fabricated and tested to be functional well by using simulated signal.

Technical trainings of the SRF project at Cornell has been proceeded including chemical cleaning of the cavity, cryostat assembling, system cool-down and warm-up handling, rf processing, and system operating.

Progress and Possible Development of the RF Gun Systems

The first photoelectron beam from the second X-band rf gun (out of the international collaboration between SRRC and UC Davis), was produced on November 21, 2000. The beam test result was published as listed in the reference. An S-band rf gun system was also constructed at SRRC. The high power modulator using the XK-5 klystron (from UC Davis through the collaboration on X-Band rf gun project) was completed and tested with high voltage charging up to 40 kV. In order to improve the single bunch purity, increase the injection efficiency, and control the filling pattern of the stored electron beam, a high-current electron source is highly desirable. A photocathode rf gun is an excellent candidate for achieving these goals. A feasibility study will be carried out using the existing rf gun system.

Commissioning of the Longitudinal Feedback System

A high-speed data-transfer problem (associated with the interface circuitry between the ADC, DSP modules, and the DAC) has been resolved. System integration was completed in June. Multi-bunch beam testing has begun. With the feedback system turned on, measurements of the beam-signal spectra demonstrate complete suppression of all longitudinal coupled-bunch modes at low beam currents (50 mA). Other evidence for the successful suppression of these modes is the significant reduction of horizontal photon-beam size as measured by the synchrotron light monitor. These data demonstrate that the digital feedback system functions as designed. Tuning up the system for high beam current operation is under way.

Instrumentation Development Division

Accelerator System and Components

1.5 GeV Upgrade

The septum magnet and the White Circuit inductors of the dipoles and the quadrupoles at the booster ring were installed in January 2000. Successful modifications on the machine components resulted in a smooth commissioning for the 1.5 GeV injector upgrade.

Temperature and Mechanical Stability

In order to study the beam orbit stability, we measured the displacement of the dipoles, quadrupoles, sextupoles, beam position monitors, and the girder structure. The measuring system was carefully designed to provide a resolution of <0.2 μm. In the R2 section, about 40 position sensors, including potentiometers and linear variable differential transformers, were installed. All signals were real-time accessed. Correlations between beam orbits and mechanical motions were observed. However, more controlled machine studies are needed to clarify some ambiguities. The sensitivity factors that relate the displacements of the beam orbits and the major components to the air and water temperature are listed in *Table 1*.

Table I The sensitivity factors of the air and the water temperature to the displacement of the beam orbit and the major component.

		Temp. Variation		Sensitivity facto	Sensitivity factor (component displ.)		
		Before	Year 2000	Beam Orbit Displ.	Girder	Magnet	BPM
1	Air Temp.	>1℃	<±0.15℃	20-100 μm/℃	10 μm/℃(Ver.)	x	x
2	Water Temp. (Magnet)	>1℃	<±0.15℃	5-50 μm/℃	x	~10 μm/℃ (Dipole-Hor.)	x
3	Water Temp. (Vacuum)	~2℃	1.5℃	>50 μm/1.5℃	x	(To be measured)	~1 μm/℃

Studies were conducted in order to reduce the temperature variations in the DI water and the air conditioning systems, in order to improve mechanical stability. Thermal deformation of the magnet girder was analyzed using the Computational Fluid Dynamic (CFD) program. The time-variant temperature distribution and the displacement of the magnet structure were preliminarily determined. We observed that the non-uniform temperature distribution, due to the turbulent airflow at the girder and the magnet support, caused the deformation of the whole structure. Although the whole flow field was not measured, the simulation results indicated that the deformation of the girder was significantly affected by the airflow.

From the study at the R2 section, we concluded that large temperature variations of the vacuum chamber, due to the synchrotron light irradiation with decaying beam currents, contributed to mechanical displacements. The capacity of the cooling system for the aluminum vacuum chamber seems insufficient for future 500 mA operations, when mechanical stability is considered. An improved scheme for heat removal will be provided to minimize the chamber deformation.

Accelerator Components

A new scraper with a rf shielding *(Figure 12)* was fabricated and installed in the straight section of the storage ring.

For better control of the electron beam orbit during gap or phase changes of the insertion devices, several correctors with horizontal and vertical fields were fabricated and installed near the U9, U5, and EPU5.6 undulators. In addition, 15 correctors were also fabricated and installed in the storage ring to provide local orbit bumps.

Utility System Upgrade

Utility Building Phase II is under construction to provide for increased utility capacity (chilled water, DI water, and electricity) required by the superconducting radiofrequency (SRF) system and the accelerator upgrade. The construction is scheduled for completion in the year 2001. A new cryogenic system will also support the SRF system.

In addition, an electrical power Supervisory Control And Data Acquisition (SCADA) system and some

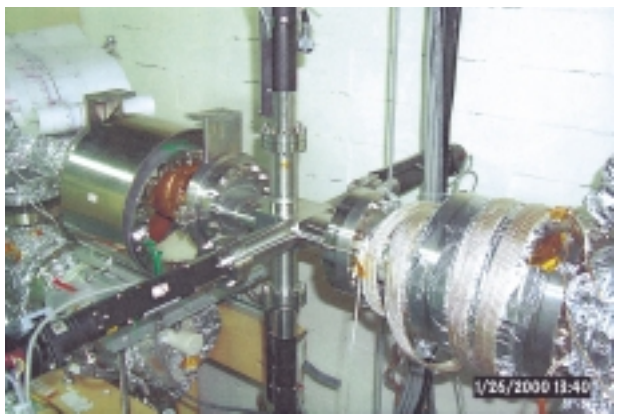

Figure 12 New scraper installed in the straight section of storage ring.

harmonic detectors were set up for real-time monitoring of the electrical quality, which is crucial for optimal machine operations. The electrical ground system has also been evaluated.

The SRRC has contracted out a liquid helium cryogenic system to Air Liquide Company. The system, which will be delivered in 2002, supplies liquid helium to the SRF cavity designed to replace the current copper cavities. *Figure 13* shows the configuration of the cryogenic system. The system consists of a 315 KW compressor, a 45 KW recovery compressor, a 10 KW refrigerator (cold box), a 2000 L dewar, two 100 m^3 gas helium storage tanks, and a 6 m multi-channel transfer line. The liquid helium will be first sent to the distribution valve box through the multi-channel transfer line, and then sent to the cryostat of the superconducting cavity through the flexible transfer line. The large power compressor is located 80 m away from the storage ring in order to minimize the effect of vibrations on the beam orbits.

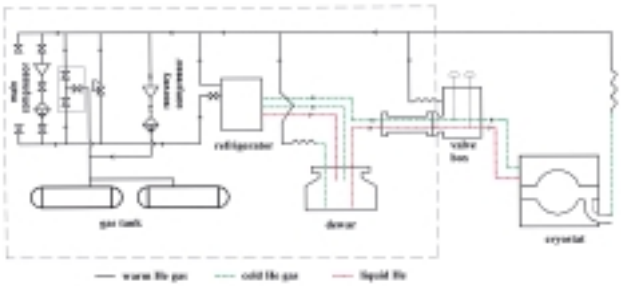

Figure 13 Flow chart of the liquid helium cryogenic system.

Insertion Devices

Superconducting Wavelength Shifter

The designs of the magnet structure, vacuum chamber and beam position monitors were completed. Bipolar power supplies, one main power with 350 A and one trim power supply with 50 A, are used to provide the 6T peak field strength and the integral field compensation. The vacuum chamber was fabricated and the beam position monitors were tested. The main magnet structure of the three-pole 6T superconducting wavelength shifter (SWLS) is under construction and will be completed by the year 2001.

Superconducting Multi-pole Wiggler

A superconducting multi-pole wiggler (SMPW) is proposed for installation at the downstream of the superconducting rf cavity. Preliminary design parameters of the SWLS and the SMPW are listed in *Table 2*. *Figure 14* shows the comparison of the brilliance of the wiggler W20, the bending magnet, SWLS, and the SMPW. The brilliance of the 1.4 m SMPW is significantly higher than that of the existing wiggler W20. Detailed design of the SMPW will be completed in the coming year.

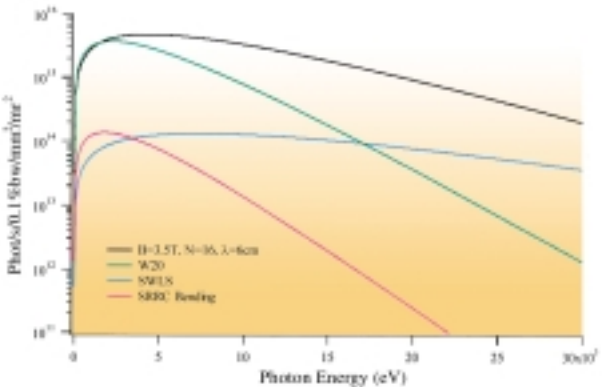

Figure 14 Photon brilliance of the wiggler W20, bending magnet, SWLS, and SMPW.

Front End and Photon Beamline Components

U9 Beamline

The installation of the U9-white light and the U9-CGM beamlines was completed in the year 2000. In addition to the typical components, gas filter systems were incorporated in the two beamlines. The gas filter for the U9-white light beamline, including the differential pumping system and the interlock system, was installed and is now in operation. The gas cell *(Figure 15)* system for the U9-CGM beamline has been successfully tested and will be installed in 2001.

Table 2 Specifications of the superconducting wavelength shifter and multipole wiggler.

	SWLS	SMPW
Number of effective period	0.5	32
Physical dimension L × W × H [cm]	83.5 × 61 × 61	140 × 120 × 208
Magnet period [cm]	23	6
Magnet Gap [cm]	5.1	1.4
Horizontal (vertical) beam aperture [cm]	10 (2)	8 (1.2)
Cryorefrigerator	cryocooler	LHe
Peak filed [T]	6.0	3.5
Reflection parameter K_x	128	19.6
Critical energy [keV]	8.98	5.24
Horizontal opening angle [mrad]	43.5	6.7
Integral dipole [G-cm]	< ± 20	< ± 20
Second integral [G-cm^2]	< ± 5000	< ± 5000
Integral quadrupole [G]	< ± 25	< ± 25
Integral sextupole [G/cm]	< ± 50	< ± 50
Integral octupole [G/cm^2]	< ± 50	< ± 50

Figure 15 Assembly test of the differential pumping system for the gas cell for 21B(U9-CGM) beamline.

IR Beamline

The aluminum vacuum chamber was successfully fabricated and installed. The chamber extracts synchrotron light with a photon span of 36 mrad in the vertical plane and 70 mrad in the horizontal plane, at a bending magnet for the infrared (IR) beamline. The front end and its interlock system were also fabricated and installed.

The mirror, the mirror bender, and the mirror manipulators were successfully fabricated, installed and operated in good condition. This IR mirror system *(Figure 16)* is the first synchrotron light mirror system developed in-house.

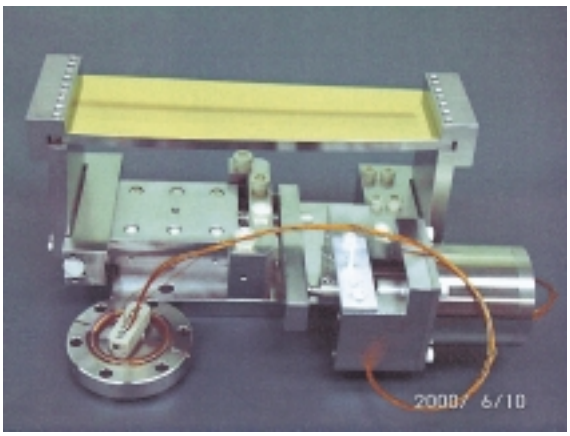

Figure 16 Horizontal K-B focusing mirror for the infrared beamline.

Photon Beam Position Monitor (PBPM)

The data acquisition system for the four vertical PBPMs at the front end FE05, FE12, FE22, and FE24 were modified. Because of the high resolution (< 0.5

μm) and because there is no mirror between the PBPM and the light source, the reading of the PBPM is used as an important index of the orbit stability of the electron beam.

Optical Technology

During the year 2000, several optical techniques were continuously developed. A bender for an active grating was manufactured. A sputtering coating system with two sputter guns and multi targets was assembled. A crystal analyzer made of high quality silicon was developed *(Figure 17)*. Some prototypes will be tested using the photon beam in 2001.

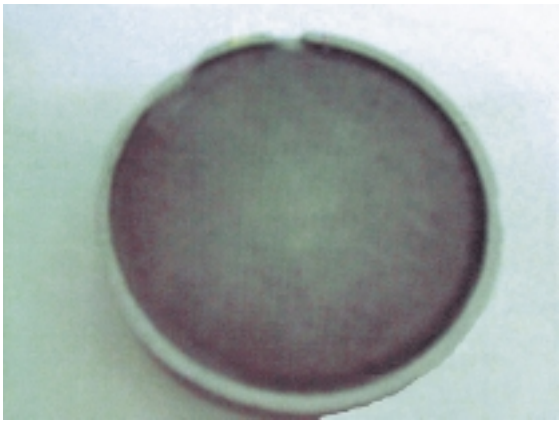

Figure 17 *Ultrahigh resolution bent crystal analyzer. A silicon disk of four inches in diameter, 3 mm in thickness, was cut into more than 7000 silicon crystals, glued to a concave optical substrate, and the crystals were kept in the original orientation.*

SPring-8 Project

The insertion device and the front end for the BL12XU beamline *(Figure 18)* have been installed and are scheduled for commissioning with the photon beamline.

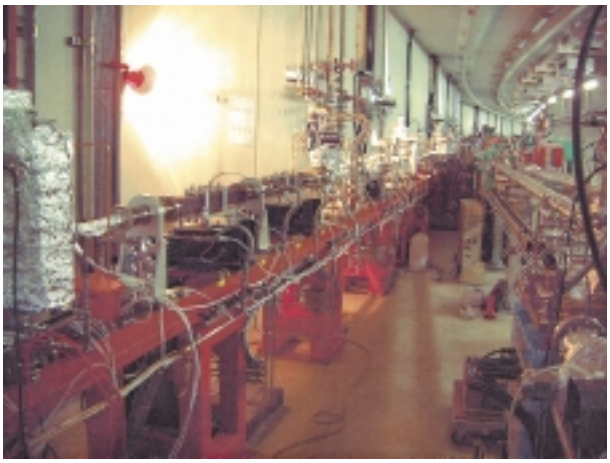

Figure 18 *Front end of the BL12XU beamline at SPring-8, Japan.*